

Provided for non-commercial research and education use.
Not for reproduction, distribution or commercial use.



This article appeared in a journal published by Elsevier. The attached copy is furnished to the author for internal non-commercial research and education use, including for instruction at the authors institution and sharing with colleagues.

Other uses, including reproduction and distribution, or selling or licensing copies, or posting to personal, institutional or third party websites are prohibited.

In most cases authors are permitted to post their version of the article (e.g. in Word or Tex form) to their personal website or institutional repository. Authors requiring further information regarding Elsevier's archiving and manuscript policies are encouraged to visit:

<http://www.elsevier.com/authorsrights>



Contents lists available at ScienceDirect

Journal of Chromatography A

journal homepage: www.elsevier.com/locate/chroma

On-line miniaturized asymmetrical flow field-flow fractionation–electrospray ionization–tandem mass spectrometry with selected reaction monitoring for quantitative analysis of phospholipids in plasma lipoproteins



Iseul Yang, Ki Hun Kim, Ju Yong Lee, Myeong Hee Moon*

Department of Chemistry, Yonsei University, 50 Yonsei-ro, Seodaemun-gu, Seoul 120-749, South Korea

ARTICLE INFO

Article history:

Received 24 September 2013

Received in revised form

14 November 2013

Accepted 14 November 2013

Available online 22 November 2013

Keywords:

Asymmetrical field-flow fractionation

Tandem mass spectrometry

AF4-ESI-MS/MS

Selected reaction monitoring

Phospholipids

Coronary artery disease

ABSTRACT

A direct analytical method for high speed quantitative analysis of lipids in human blood plasma using on-line chip-type asymmetrical flow field-flow fractionation–electrospray ionization–tandem mass spectrometry (cAF4-ESI-MS/MS) with selected reaction monitoring (SRM) is described in this study. Utilizing a miniaturized cAF4 channel, high speed size separation of high density lipoproteins (HDL) and low density lipoproteins (LDL) from plasma samples can be accomplished at a microflow rate along with simultaneous desalting of lipoproteins, both of which are conducive to direct ESI of lipids in lipoproteins. This study demonstrates that the SRM method to monitor phospholipids during cAF4-ESI-MS/MS can be successfully applied to the quantitation of lipid molecules in plasma lipoproteins without the need of a separate lipid extraction process. For quantitation of lipids in HDL and LDL during cAF4-ESI-MS/MS runs, a protein standard (carbonic anhydrase, 29 kDa) was added to each plasma sample as an internal standard such that a peak intensity of y_{67}^{+5} ions, which are high abundant SRM product ions of CA, could be utilized to calculate the relative intensity of each lipid molecule. The developed method was applied to plasma samples from 10 patients with coronary artery disease (CAD) and 10 healthy control samples, and quantitative analysis of 39 lipid molecules including phosphatidylcholines, phosphatidylethanolamines, sphingomyelins, phosphatidylglycerols, and phosphatidylinositols, resulted in the selection of 13 PL species showing more than 2.5 fold difference in relative abundance ($p < 0.01$) between the groups. The present study demonstrates a high speed analytical method for determining plasma lipid content and distribution without an organic solvent extraction of lipids from plasma.

© 2013 Elsevier B.V. All rights reserved.

1. Introduction

Flow field-flow fractionation (FIFFF) is a family of versatile size fractionation methods applicable to proteins, water soluble macromolecules, nanoparticles, and cells that operates by the application of a hydrodynamic force (crossflow) to sample components perpendicular to the migration flow in an empty FIFFF channel [1–4]. Due to differences in diffusion coefficients, sample components of different sizes are differentially distributed against the rectangular or cylindrical channel wall of FIFFF, and they migrate at different velocities along the channel axis providing that a parabolic migration flow profile is delivered. Therefore, separation is achieved in order of increasing size. Since retention in FIFFF can be clearly predicted by theory [5], FIFFF has been readily utilized for the study of

qualitative information such as diffusion coefficient, particle size, and particle size distribution, and together with on-line light scattering measurements for molecular weight distribution.

Lipids in human blood are carried via lipoproteins, which are globular complexes containing fats and cholesteryl esters (CEs) in the core and proteins along with lipids at the surface [6]. Since coronary artery disease (CAD) is known to be related to low levels of high density lipoprotein (HDL) and the size decrease of low density lipoprotein (LDL) [7–9], it is important to understand the composition and concentration distribution of lipid species in HDL and LDL for clinical purposes such as diagnosis and monitoring of therapeutic progress. Among lipids, phospholipids (PLs) are major lipoprotein components, and their molecular structures are complicated by combinations of different head groups and acyl chains of differing lengths and degree of unsaturation. Due to the complicated nature of PLs, PL analysis requires high resolution separation of PLs along with sophisticated MS detection. However, this process requires three steps to analyze plasma lipids when HDL/LDL

* Corresponding author. Tel.: +82 2 2123 5634; fax: +82 2 364 7050.

E-mail addresses: mhmoon@yonsei.ac.kr, mhmoon@hotmail.com (M.H. Moon).

specific lipids are to be examined: size fractionation or isolation of HDL and LDL particles either by density gradient ultracentrifugation (DGU) [10,11] or polyacrylamide gel electrophoresis (PAGE) [12], extraction of lipids from each lipoprotein fraction using an organic solvent mixture [13,14], and MS analysis using matrix-assisted laser desorption and ionization (MALDI) [15] or electrospray ionization (ESI) interfaced with liquid chromatography (LC–ESI–MS) [16–18].

FIFFF has shown the capability of size fractionation of HDL and LDL from human blood plasma with selective detection using Sudan Black B staining [19] or fluorescence labeling [20] and MALS [21]. A miniaturized FIFFF was utilized to determine size of purified lipoprotein particles and to study aggregation behaviors of LDL upon external stimuli [22]. Semipreparative separation of lipoproteins can be readily achieved using multiplexed hollow fiber FIFFF (MxHF5) for the collection of HDL/LDL fractions from which PLs can be analyzed by nanoflow LC–ESI–MS/MS [23,24]. In this case, lipids had to be extracted from the lipoprotein fraction using organic solvents. Recently, it was demonstrated that chip-type miniaturized asymmetrical FIFFF (cAF4) could be on-line coupled with ESI–MS (cAF4–ESI–MS) for possible top-down lipid analysis [25]. The latter study showed potential as HDL/LDL particles eluted from cAF4 could be directly infused to a MS via ESI, and the effect of on-line sample desalting during FIFFF separation enhanced the direct ionization and characterization of lipid molecules of LDL standards in cAF4–ESI–MS/MS. While the previous study [25] showed the possibility of detecting several PLs, triacylglycerols (TGs), and CE molecules, a proper quantification method was not developed due to the lack of a proper internal standard, which would be needed for the analysis of the variation of target lipid molecules between patients and healthy control samples. The addition of an external lipid standard to plasma samples was not practical due to poor lipid solubility, and moreover, added lipid standard molecules if dispersed in the plasma sample would not be retained in the FIFFF channel due to their small size. Though an added lipid standard could be bound to the lipoprotein particle surface, the concentration level for lipid detection would not be consistent due to the size variation of lipoprotein particles.

This study expands the capability of FIFFF for the quantitative analysis of lipids in human blood plasma using cAF4–ESI–MS/MS with the selected reaction monitoring (SRM) method. SRM was applied to cAF4–ESI–MS/MS for quantifying phospholipids during the separation of HDL/LDL by cAF4 followed by direct ionization of lipids contained in lipoproteins aided by in-source fragmentation. Instead of measuring the peak area of each lipid precursor ion, quantitation of lipid molecules by cAF4–ESI–MS/MS was accomplished by monitoring the peak area of the characteristic fragment ion of the lipid during the SRM transition. Validation of the peak area calculation of SRM product ions for various lipids was attained with repeated cAF4–ESI–MS/MS analysis of a human plasma sample. To calculate the relative MS intensity of a class-specific product ion from lipid, a small protein internal standard, carbonic anhydrase (CA, 29 kDa), was added to the plasma sample such that the SRM product ion, a high abundant fragment ion, was detected during the SRM transition (m/z 1613.3 for $[M+18H]^{+18} \rightarrow 1521.2$ for multiply charged peptide fragment ion y_{67}^{+5} in positive ion mode) to obtain the relative intensity of each lipid molecule to compensate for possible variations in cAF4 separation. The effect of the protein internal standard on the ionization of lipid molecules was investigated with lipoprotein as well as SRM based quantitation of lipids with different cAF4 run conditions to vary the degree of peak overlap of CA with HDL. The cAF4–ESI–MS/MS with SRM was further applied to the quantitative analysis of 13 phosphatidylcholines (PCs), 8 phosphatidylethanolamines (PEs), 3 sphingomyelins (SMs), 12 phosphatidylglycerols (PGs), and 3 phosphatidylinositols (PIs) of

both HDL and LDL from 10 CAD patient and 10 healthy control plasma samples to distinguish PL species with significantly different amounts in patients.

2. Experimental

2.1. Materials and reagents

All chemicals were purchased from Sigma (St. Louis, MO, USA): HCO_2H , NH_4OH , NH_4HCO_2 , NH_4HCO_3 , and CH_3CN . Human blood plasma samples from CAD patients and healthy controls were obtained with written consent from the Yonsei University School of Medicine. Plasma samples were injected into the cAF4 after depletion of albumin and IgG using a depletion spin column from Sigma in order to reduce ionization suppression. For depletion, the spin column kit was first equilibrated with 22 mM Tris–buffer (pH 7.4). Each plasma sample, diluted in the same buffer, was placed in the spin column for centrifugation at $5000 \times g$ for 1 min, and then the eluate was reapplied to the same spin column for 10 min. Finally, the filtrate was washed with 200 μL of Tris–buffer (pH 7.4) and then stored for analysis.

2.2. cAF4–ESI–MS/MS

The cAF4 channel utilized in this study was basically the same as the previous model [25] except that one 3 mm-thick acryl plate was inserted as a depletion wall of the FIFFF channel (above the channel spacer) to provide metal-free pathway for biomaterials and to avoid possible channel leaking. The cAF4 channel was constructed with four 1.5 mm-thick stainless steel (SS) plates and a 3.0 mm-thick acryl block as shown in Fig. 1. Two plain plates at the top and bottom sides were binding blocks to clamp a series of layers in the following order: acryl block, 150 μm -thick PVC channel spacer cut in a rectangular design (0.5 cm wide and 7.2 cm long), regenerated cellulose membrane with a molecular mass cut-off of 10 kDa (Wyatt GmbH, Dernbach, Germany), SS layer embedded with a 1.5 mm-thick stainless frit (10 cm \times 1.5 cm \times 0.15 cm, 5 μm pore size) in the center, and another SS layer to provide flow reservoir space cut in a rectangular design (9.6 cm \times 1.1 cm \times 0.15 cm). The total thickness of the cAF4 channel was slightly over 9 mm. The inlet and outlet ports of the cAF4 were made by drilling two holes in the top SS plate, and two nanoport assemblies from Upchurch Scientific (Oak Harbor, WA, USA) were thermally fixed on top of both drilled ports. Flow connections were made with capillary tubing (360 μm -o.d. and 200 μm -i.d.).

Carrier solutions for cAF4 separation were prepared with deionized water ($>18 M\Omega$) according to the ionization mode of ESI–MS: 10 mM NH_4HCO_3 solution for positive ion mode and 5 mM ammonium formate (NH_4HCO_2) for negative ion mode. For the delivery of carrier solution to the cAF4, a model SP930D HPLC pump from Young-Lin (Seoul, Korea) was utilized through a model 7725 loop injector with a 20 μL loop from Rheodyne (Cotati, CA, USA). The focusing/relaxation of injected sample components was effected at a position one-fifth of the channel length from the inlet, and at least 2 min under the crossflow rate (400 $\mu L/min$) was allowed for focusing/relaxation after sample injection. The outflow rate (16 $\mu L/min$) of the cAF4 was split via a MicroTee from Upchurch Scientific using a syringe pump in un-pump mode (for accurate control of feed flow rate to MS) shown in Fig. 1, a model Legato 110 syringe pump from KD Scientific (Holliston, MA, USA) for waste, and the rest of the flow (6 $\mu L/min$) was mixed with ionization modifier liquid (1% formic acid in CH_3CN for positive ion mode or 0.5% NH_4OH for negative ion mode of MS analysis) delivered from a syringe pump equipped in the MS system at a flow rate of 5 $\mu L/min$ exiting to the ESI emitter. The final feed rate to the ESI–MS was 11 $\mu L/min$. For

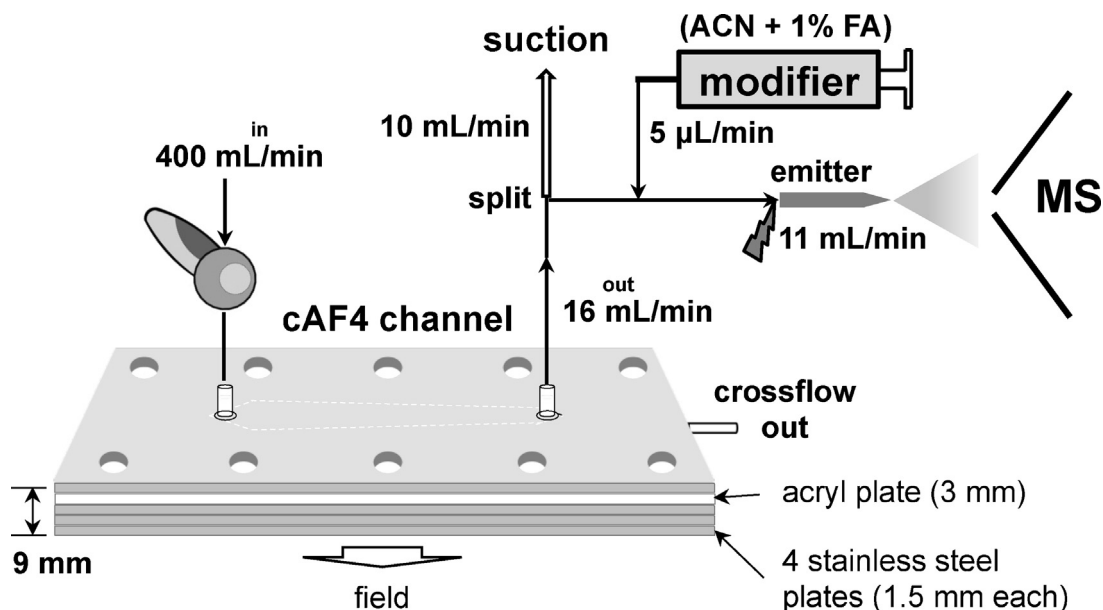


Fig. 1. Schematic of cAF4-ESI-MS/MS for lipid analysis from plasma lipoproteins. To split the outflow from the cAF4 channel, a syringe pump in un-pump mode was utilized. Mixing of modifier liquid was performed with another syringe pump at a flow rate of 5 $\mu\text{L}/\text{min}$, in total 11 $\mu\text{L}/\text{min}$ of flow was fed to the MS via ESI.

mixing the cAF4 outflow with ionization modifier liquid, a Microcross from Upchurch Scientific was utilized. For the ESI emitter, a pulled tip capillary tube prepared by pulling one end of a capillary tip (9.5 cm \times 200 μm i.d., 360 μm o.d.) with a flame to make a sharp needle was used.

ESI of lipid ions was performed by applying 3.0 kV with the capillary temperature set at 200 $^{\circ}\text{C}$ through a Pt wire inserted in the Microcross, and the in-source fragmentation method was applied with 40V in order to enhance dissociation of lipoprotein particles and to reduce the passage of multimeric lipid ions. Collision induced dissociation (CID) for MS/MS in SRM mode was achieved with 40% of the normalized collision energy. The range of m/z was 400–2000 for precursor and 300–2000 for CID runs. The mass tolerance between the measured mono-isotopic mass and the calculated mass for the identification of lipids was set to 1.0 Da. MS data acquisition was carried out with Xcalibur software from Thermo Fisher Scientific. PL molecules of lipoproteins to be examined for SRM of cAF4-ESI-MS/MS were from previous results obtained by data dependent CID analysis using nLC-ESI-MS/MS [24]. The m/z lists of precursor and quantifier ions for targeted PL molecules were included in the Xcalibur software for m/z specific SRM analysis. The quantifier ion of an internal standard protein (CA) was selected from a high abundant CID fragment from experiments (confirmed with the calculated y-type fragment ion m/z from its amino acid sequences in Uniprot database (<http://www.uniprot.org/>)) as m/z 1613.3 for $[\text{M}+18\text{H}]^{+18} \rightarrow 1521.2$ for y_{67}^{+5} , multiply charged peptide fragment ion in positive ion mode and m/z 1318.4 for $[\text{M}-22\text{H}]^{-22} \rightarrow 1270.9$ for y_{78}^{-7} in negative ion mode. Types of SRM quantifier ions for PLs are listed in Table 1.

3. Results and discussion

Quantitative analysis of PLs during the separation of HDL/LDL from human blood plasma samples using cAF4-ESI-MS/MS with SRM method requires consistent ionization of a selected quantifier ion. In order to adopt the SRM method with cAF4-ESI-MS/MS, the ionization stability of a selected quantifier ion in each PL category was evaluated in repeated cAF4-ESI-MS/MS runs. Fig. 2a shows superimposed SRM fractograms ($n=5$) of a plasma sample obtained by cAF4-ESI-MS/MS. Each fractogram was based on the detection of 36:4-PC which was obtained by extracting the peak intensity of the product ion m/z 599.6 ($[\text{M}+\text{H}-183]^{+}$) from the SRM transition of the precursor ion m/z 782.6 ($[\text{M}+\text{H}]^{+}$), hereafter represented as the SRM transition of m/z 782.6 \rightarrow 599.6. Each SRM fractogram in Fig. 2a was plotted with the relative intensity of the SRM quantifier ion to that of an internal standard (IS), carbonic anhydrase (CA, 29 kDa), which was added to the plasma sample at a concentration of 0.2 $\mu\text{g}/\mu\text{L}$ to compensate for variations in cAF4 separation and MS detection. Fig. 2a was obtained with a 2.5 μL plasma sample containing 0.5 μg of CA for each injection. In this case, the quantifier ion for CA was selected from the SRM transition of m/z 1613.3 \rightarrow 1521.4, which was the most intense peptide fragment ion (y_{67}^{+5}) of the multiply charged protein ion ($[\text{M}+18\text{H}]^{+18}$). This will be discussed in greater detail later. The flow rate of Fig. 2a was 0.40/0.016 mL/min of inflow/outflow rate ($\dot{V}_{in}/\dot{V}_{out}$). Fig. 2b and c shows the precursor scans obtained during $t_r=3.6\text{--}3.9$ min from cAF4-ESI-MS and MS/MS spectra of the targeted precursor ion m/z 782.6 by CID, respectively. The product ion $[\text{M}+\text{H}-183]^{+}$ was selected as the SRM quantifier ion for PC species since it is a characteristic fragment from cleavage of the phosphocholine head group ($\text{HPO}_4(\text{CH}_2)_2\text{N}(\text{CH}_3)_3$, 183 Da) from PC during the CID experiment, which was the most intense among fragment ions that are formed by loss of each acyl chain in the form of ketene ($[\text{M}+\text{H}-\text{R}'\text{CH}=\text{C}=\text{O}]^{+}$, 544.5 and 496.4) and carboxylic acid ($[\text{M}+\text{H}-\text{RCOOH}]^{+}$, 526.5 and 478.4). The subscripts 1 and 2 in the acyl chain R in Fig. 2c denote the acyl chain location as sn-1 and sn-2 on the glycerol backbone of the PL molecule, respectively. Typically from CID spectra of PC, the acyl chain location can be identified from the intensity difference between the fragment ions after loss of an acyl chain since dissociation of an acyl chain in the form of ketene from the sn-2 position

Table 1

List of SRM quantifier ion types in cAF4-ESI-MS/MS analysis to detect PLs in lipoproteins.

Class	Examined species	Description of SRM	Ionization mode
PC	13	$[\text{M}+\text{H}]^{+} \rightarrow [\text{M}+\text{H}-183]^{+}$	Positive
PE	8	$[\text{M}+\text{H}]^{+} \rightarrow [\text{M}+\text{H}-141]^{+}$	Positive
SM	3	$[\text{M}+\text{HCOO}]^{-} \rightarrow [\text{M}-\text{CH}_3]^{-}$	Negative
PG	12	$[\text{M}-\text{H}]^{-} \rightarrow [\text{RCOO}]^{-}$	Negative
PI	3	$[\text{M}-\text{H}]^{-} \rightarrow [\text{M}-\text{H}-\text{RCOOH}]^{-}$	Negative

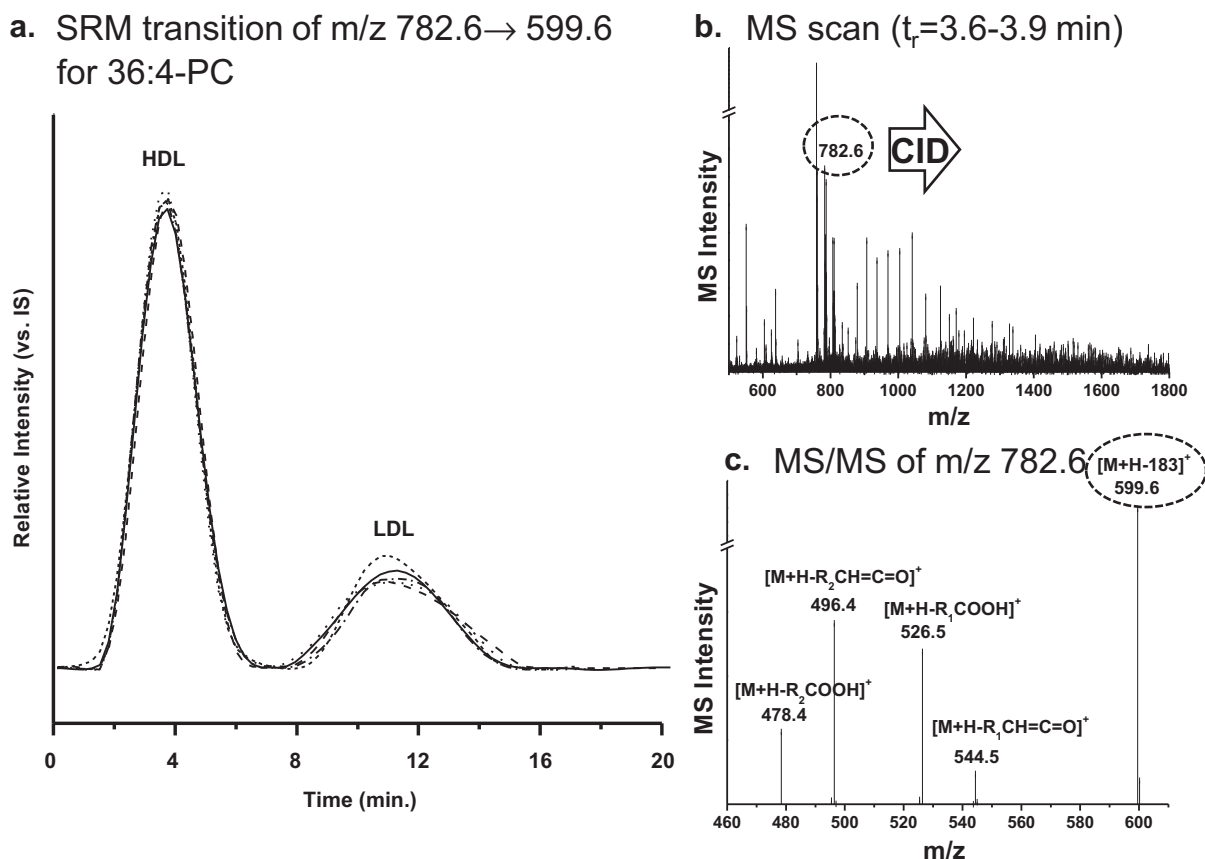


Fig. 2. (a) Superimposed SRM fractograms obtained by cAF4-ESI-MS/MS of 36:4-PC (SRM transition of m/z 782.6 ($[M+H]^+$) \rightarrow m/z 599.6 ($[M+H-183]^+$)) from 5 repeated injections of a healthy human plasma sample along with (b) MS spectra obtained during $t_r = 3.6$ – 3.9 min and (c) the corresponding MS/MS spectra of the precursor ion m/z 782.6 showing characteristic fragment ion spectra of 36:4-PC. The product ion $[M+H-183]^+$ representing loss of the phosphocholine head group (183 Da) was selected as the SRM quantifier ion for all PC molecules.

is more preferable than from sn-1 [26]. The CID spectra of Fig. 2c provided information that the precursor ion (m/z 782.6) contained two acyl chains as 16:0 and 20:4 (representing the number of carbons and double bonds in the acyl chain); however, when the SRM quantifier ion for PC was selected as $[M+H-183]^+$, it was possible to detect all of the isobaric PC species such as 18:1/18:3-PC, 18:2/18:2-PC, and 16:0/20:4-PC. Therefore, the molecular structure of PCs in this experiment is expressed with the total carbon numbers and double bonds as 36:4-PC for Fig. 2a.

Quantifier ions for the detection of other lipids during cAF4-ESI-MS/MS analysis are listed in Table 1. Phosphatidylethanolamine (PE) was detected with the SRM transition of $[M+H]^+ \rightarrow [M+H-141]^+$, which represents the loss of phosphoethanolamine ($\text{HPO}_4(\text{CH}_2)_2\text{NH}_3$, 141 Da) in positive ion mode. For sphingolipid (SM), which was detected in negative ion mode for the SRM transition of the formate adduct ion $[M+\text{HCOO}]^- \rightarrow [M-\text{CH}_3]^-$, the typical loss of a methyl group was selected. For phosphatidylglycerol (PG) and phosphatidylinositol (PI), free carboxylate ion ($[\text{RCOO}]^-$) and the fragment ion ($[M-\text{H}-\text{RCOOH}]^-$) produced by loss of the acyl chain in the form of carboxylic acid from each precursor ion ($[M-\text{H}]^-$) were selected as the SRM quantifier ions, respectively. The total number of identified lipids in each PL category is listed in Table 1, and the molecular structures are included in Table S1 of the Supplementary Information.

With the addition of an internal standard (IS), fractograms plotted from the relative intensity of the SRM quantifier ion in Fig. 2a shows that good reproducibility in the detection of HDL and LDL by cAF4-ESI-MS/MS was achieved along with complete baseline

separation within 16 min: average values of retention time and peak area were 3.71 ± 0.07 min (19.27 ± 0.14 for peak area) and 11.21 ± 0.14 min (6.81 ± 0.36) for HDL and LDL, respectively ($n = 5$). CA was chosen as the internal standard for the following reasons. Since molecular weight cut-off of the channel membrane used for cAF4 was 10 kDa, simple addition of a lipid standard to the plasma sample was not effective. In the case of a large macromolecule as internal standard, a protein that is retained by lipoprotein particles would be desirable. Though CA exists in human blood plasma, the average peak area of CA measured from control samples was 0.00 ± 0.01 ($n = 3$), which is very low compared to 193.91 ± 2.98 ($n = 3$), based on the peak area measurement of added CA ($0.5 \mu\text{g}$ for each injection) to each sample. Therefore, the effect of natural CA in plasma on quantitation was assumed to be negligible.

With CA as an IS, there was a concern with the influence of peak overlap of CA with HDL during the ionization of lipids for quantification of a targeted PL from HDL. Fig. 3a shows the superimposed SRM fractograms of 34:2-PC from HDL of the same plasma sample based on the SRM transition m/z 758.7 \rightarrow 575.7 and added CA molecules based on the SRM of m/z 1613.3 ($[M+18\text{H}]^{+18}$) \rightarrow 1521.4 (y_{67}^{+5}). The MS signal of the plasma sample after 10 min is not shown in Fig. 3a. The MS spectra shown in Fig. 3b are the accumulated precursor scans obtained in the time interval of $t_r = 1.9$ – 2.2 min, which show multiply charged protein ion peaks of CA among which a precursor ion $[M+18\text{H}]^{+18}$, was selected for the MS/MS experiment (the resulting CID spectra shown in Fig. 3c) since the MS baseline around the $[M+18\text{H}]^{+18}$ ion was relatively less noisy and was far from the m/z region of most lipid species (<1200 m/z). As shown in Fig. 3c, the fragment ion y_{67}^{+5} (m/z 1521.4) was selected as the quantifier ion

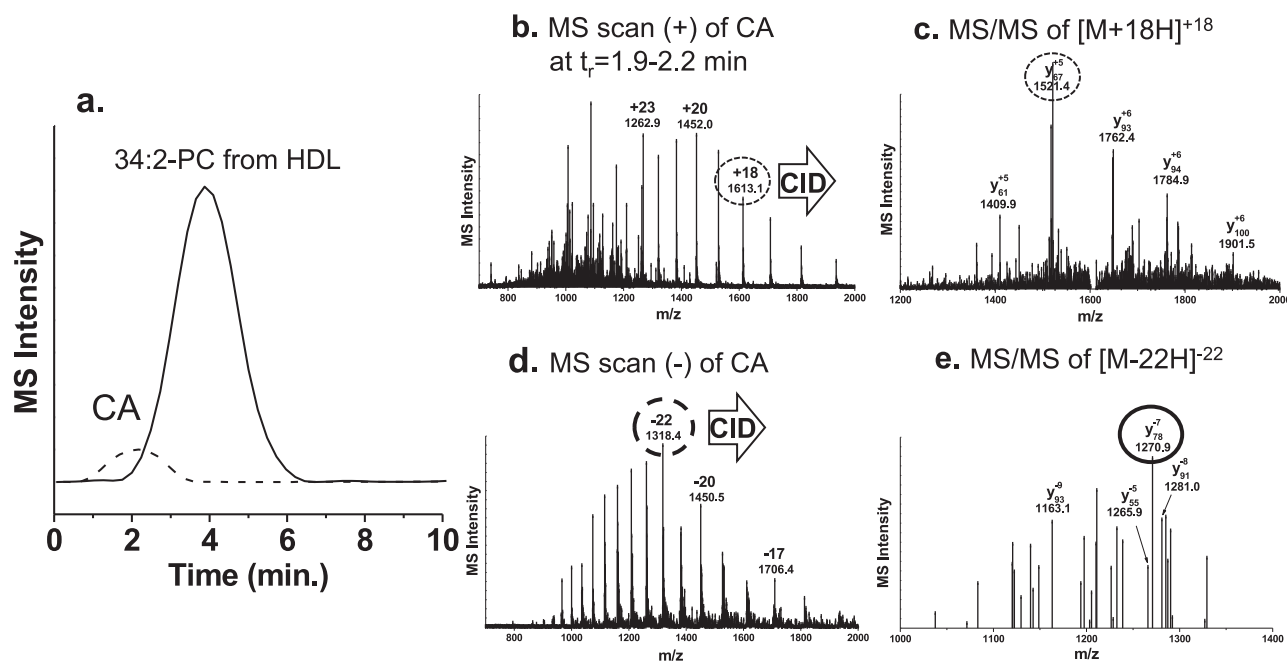


Fig. 3. (a) SRM fractograms of 34:2-PC from HDL of a plasma sample (2.5 μ L) based on the SRM transition of m/z 758.7 \rightarrow 575.7 overlapped with the SRM fractogram of CA, an internal standard (0.5 μ g), based on m/z 1613.1 ($[M+18H]^+_{18}$) \rightarrow 1521.4 (y_{67}^{+5}), (b) MS spectra of CA during $t_r = 1.9$ –2.2 min in positive ion mode, (c) MS/MS spectra of $[M+18H]^+_{18}$, (d) MS spectra of CA in negative ion mode, and (e) MS/MS spectra of $[M-22H]^{-22}$ (m/z 1318.4).

for CA since it had the strongest intensity among the peptide fragment ions. In Fig. 3a, 42.5% of the CA peak overlapped with the HDL peak based on 34:2-PC. The degree of CA overlap with HDL based on SRM fractograms may appear to be different from lipids since the concentration of individual lipid species in HDL particles will vary. The relative peak intensity of 34:2-PC to CA was obtained from the intensity of the SRM quantifier ion ($[M+H-183]^+$) of 34:2-PC at each retention time divided by the fixed intensity of y_{67}^{+5} obtained at the peak maximum time of CA, and the resulting relative peak area of 34:2-PC (vs. y_{67}^{+5}) in Fig. 3a was calculated to be 10.14 ± 0.31 ($n=3$) with 3% variation between runs. The flow rate conditions used for Fig. 3a were $\dot{V}_{in}/\dot{V}_{out} = 0.40/0.013$ in mL/min. When the run conditions of cAF4 were changed to $\dot{V}_{in}/\dot{V}_{out} = 0.60/0.02$ in mL/min (fractogram not shown), the degree of overlap between the two peaks was reduced to 20.0% due to the increase in the field strength of cAF4 (crossflow rate was increased from 0.387 to 0.58 mL/min), resulting in a slightly higher relative peak area of 34:2-PC of 10.48 ± 0.46 ($n=3$). The relative difference in peak overlap between the two run conditions was 3.24%. The effect of peak overlap on ionization efficiency of lipids in HDL was examined by calculating the relative difference in peak overlap between the two cAF4 run conditions for the other six lipids listed in Table 2 besides 34:2-PC: 34:3-PC, 34:1-PC, 38:4-PC, 36:3-PE, 38:6-PE, and 40:5-PE. All seven lipid species represent a broad range of abundance based

on relative peak area values (about 2–36 times); however, the relative difference between the two run conditions was $3.77 \pm 1.71\%$ for an average of 7 species in Table 2, showing that ionization efficiency of lipid species was not significantly affected by the current degree of peak overlap. When PL molecules such as SM, PG, and PI were monitored in negative ion mode, the SRM quantifier ion of IS (CA) with the most intense fragment ion during the SRM transition of m/z 1318.4 ($[M-22H]^{-22}$) \rightarrow 1270.9 (y_{78}^{-7}) was selected. The precursor scan in negative ion mode and the corresponding MS/MS spectra are shown in Fig. 3d and e, respectively.

The SRM method to quantify lipid species in HDL/LDL was applied to human plasma samples with CAD and control samples (10 each). Fig. 4 shows superimposed SRM fractograms of (a) d18:1/22:0-SM (SRM transition of m/z 831.8 \rightarrow 771.8 for $[M-CH_3]^-$) from three control and three patient samples, and (b) 38:4-PE (SRM transition of m/z 768.7 \rightarrow 627.7 for $[M+H-141]^+$) obtained with the same flow rate conditions used in Fig. 3a. For SM molecules, the chain locations of SM can be clearly distinguished as d18:1/22:0 due to the different types of chain structures: sphingosine (d18:1) and a fatty acid through an amide bond. SRM fractograms show a clear separation of HDL and LDL particles along with some variations in retention time of LDL particles among individual samples in both the control and patient samples. The retention time of LDL particles together with MS intensity of lipid

Table 2
Comparison of relative peak areas of each lipid and ratio of peak areas of lipids in HDL to CA between two different cAF4-ESI-MS/MS run conditions. The percentage of overlap represents overlapped peak areas of CA with HDL. Peak area calculation of CA was based on the SRM fractogram of y_{67}^{+5} m/z 1521.2 from the precursor ion $[M+18H]^+_{18}$ (m/z 1613.3) ($n=3$).

Class	Molecular species	m/z	$\dot{V}_{in}/\dot{V}_{out}$	0.40/0.013 mL/min		$\dot{V}_{in}/\dot{V}_{out}$		Relative difference %
				Area of HDL/CA	% CA overlapped with HDL	Area of HDL/CA	% CA overlapped with HDL	
PC	34:3	756.7	5.59 ± 0.28	30.95	5.83 ± 0.17	19.31	4.12	
	34:2	758.7	10.14 ± 0.31	42.51	10.48 ± 0.46	20.01	3.24	
	34:1	760.7	3.44 ± 0.10	28.91	3.52 ± 0.08	14.21	2.27	
	38:4	810.6	34.65 ± 0.94	43.78	36.75 ± 1.63	21.35	5.72	
PE	36:3	742.8	1.92 ± 0.08	21.42	2.04 ± 0.07	4.70	5.88	
	38:6	764.7	14.65 ± 0.48	34.91	15.26 ± 0.67	6.93	4.00	
	40:5	794.5	3.41 ± 0.12	29.26	3.56 ± 0.10	9.53	4.21	

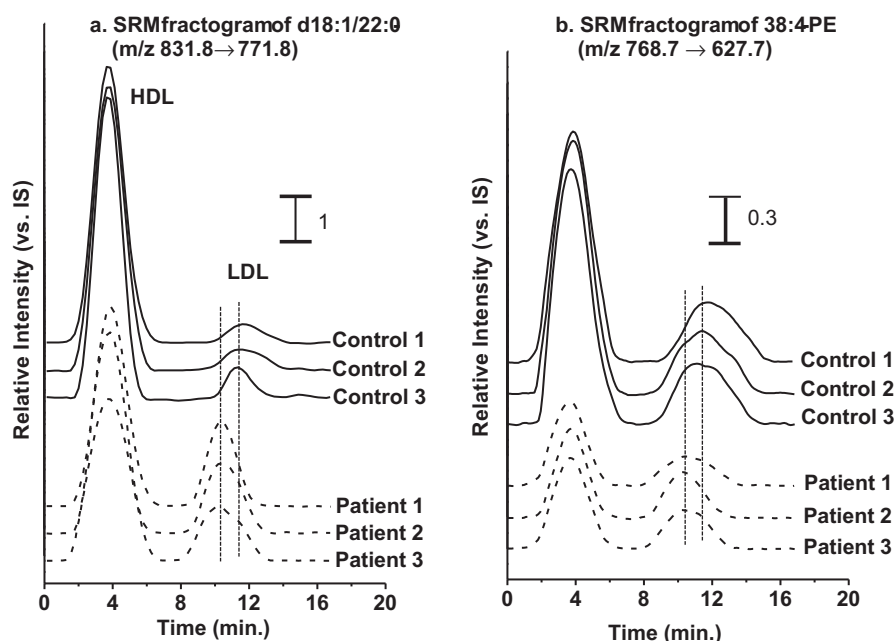


Fig. 4. Comparison of SRM fractograms based on (a) d18:1/22:0-SM (m/z 831.8 \rightarrow 771.8) and (b) 38:4-PE (m/z 768.7 \rightarrow 627.7) from three controls and three patient samples.

species obviously decreased with patient samples, reflecting a substantial decrease in LDL size (from 25.7 ± 0.5 to 23.6 ± 0.3 nm based on theoretical calculations) for CAD patients. Moreover, the decrease of HDL levels based on both lipid species was clearly observed with CAD patients in both Fig. 4a and b. However for LDL, the d18:1/22:0-SM species in Fig. 4a appear to increase significantly, while the 38:4-PE species in Fig. 4b decreased with CAD patients. These results show the variation of lipid composition in LDL particles during the development of CAD. From cAF4-ESI-MS/MS with the SRM method, 13 PCs, 8 PEs, 3 SMs, 12 PGs and 3 PIs were quantitatively examined, and the relative changes (vs. IS) in the level of each species between patients and controls are listed in Table S1 of the Supporting Information. Among the 39 PL species examined in this study, the relative amounts of most PL species exhibited notable decreases in patient HDL, while six PGs with acyl chains with combinations of 16:1, 16:2, 18:0, and 18:1 showed increases. Considering the typical decrease in HDL level

for CAD patients, these 6 PG species could be expected to exhibit a significant increase in relative concentration. Among the PLs listed in Table S1, species which met the criteria of greater than a 2.5-fold change in relative peak area of SRM quantifier ions as well as Student's *t*-test *p*-values less than 0.01 are listed in Table 3 (plotted in Figure S1 of the Supporting Information). It was found that 4 PEs and 1 PG showed an approximate three-fold decrease in their amount in patient HDL. While 2 SMs, 4 PGs, and 2 PIs exhibited a 3–13 fold increase in patient LDL, 2 PEs showed a large decrease (more than 5 fold). Though the PL species listed in Table 3 show greater than 2.5 fold changes, most have similar peak area values in relative peak area (less than 0.50 in comparison to added CA) except for a few relatively high abundant species as follows: 36:3-PE and 36:2-PE showed a significant decrease (>5-fold) in both patient HDL/LDL, 38:4-PE in patient HDL only. d18:1/18:0-SM, d18:1/22:0-SM, and (18:0, 20:4)-PI were relatively high abundant species that showed large increases (3.5–5.0 folds) in patient LDL. Moreover, the three

Table 3

Variation in the relative peak area (vs. IS) of lipid species in HDL/LDL from 10 control and 10 patient plasma samples by cAF4-ESI-MS/MS. Selection was based on species showing greater than 2.5-fold change between control and patient with $p < 0.01$ of the Student *t*-test.

Class	Molecular species	Precursor m/z	SRM m/z	Control (vs. CA)	Patients (vs. CA)	P/C	Student's <i>t</i> -test <i>p</i> -value
<i>From HDL</i>							
PE	36:3	742.8	601.8	1.80 ± 0.42	0.32 ± 0.07	0.18	<0.01
	36:2	744.8	603.8	2.77 ± 1.15	0.39 ± 0.16	0.14	<0.01
	38:4	768.7	627.7	5.44 ± 1.23	1.78 ± 0.58	0.33	<0.01
	40:3	798.8	657.8	0.46 ± 0.12	0.14 ± 0.06	0.31	<0.01
PG	18:2,18:2	769.6	279.4	0.34 ± 0.07	0.12 ± 0.08	0.36	<0.01
Apo-A1		1081.2 ^a	864.3 ^b	4.27 ± 0.50	1.71 ± 0.46	0.40	<0.01
<i>From LDL</i>							
PE	36:3	742.8	601.8	0.63 ± 0.17	N.D.	0.00	N/A
	36:2	744.8	603.8	1.43 ± 0.51	0.31 ± 0.09	0.21	<0.01
SM	d18:1/18:0	775.8	715.5	0.38 ± 0.12	1.91 ± 0.75	5.01	<0.01
	d18:1/22:0	831.8	771.7	1.06 ± 0.17	3.72 ± 0.74	3.52	<0.01
PG	16:1,18:1	745.7	281.5	0.11 ± 0.08	0.32 ± 0.13	2.96	<0.01
	18:1,18:2	771.6	279.4	0.13 ± 0.07	0.48 ± 0.21	3.59	<0.01
	16:1,20:2	771.6	307.5	0.04 ± 0.03	0.15 ± 0.08	3.68	<0.01
	18:0,18:1	775.8	283.5	0.02 ± 0.01	0.09 ± 0.06	4.63	<0.01
	PI	16:0,18:1	835.6	579.22	0.02 ± 0.02	0.20 ± 0.09	13.29
	18:0,20:4	885.7	581.19	0.39 ± 0.13	1.68 ± 0.71	4.35	<0.01

^a m/z of $[M+26H]^{+26}$.

^b m/z of y_{178}^{+24} .

SM species in the patient HDL did not decrease (0.8–0.9 fold in P/C) as much as other PC and PE species, which supports the observation that the concentration of SM species compared to other lipid species in HDL relatively increases. This result is analogous to a report [27] featuring an enzymatic method that indicated the human plasma SM level is a risk factor for CAD manifest as a significant increase in CAD patient SM levels. Another interesting finding in this study was the comparison of levels of apolipoprotein-AI (Apo AI), a major protein component of HDL that helps clear cholesterol from arteries, in CAD patients. In this experiment, Apo AI was found exclusively in HDL. The relative amount of Apo AI in HDL based on the SRM transition of $[M+26H]^{+26}$ (m/z 1081.2) \rightarrow y_{178}^{+24} (m/z 864.3) decreased 2.5 fold for CAD patients as shown in Table 3, and the corresponding SRM fractogram of Apo AI along with CID spectra of the precursor ion m/z 1081.2 are shown in Figure S2 of the Supporting Information. This result could potentially be utilized for an intervention study to monitor the variation of Apo AI of patients upon therapeutic treatment without having to rely on complicated bottom-up quantitative proteomic analysis.

4. Conclusions

The current study demonstrates that top-down lipidomic analysis using cAF4-ESI-MS/MS with SRM can be utilized to quantitatively monitor the variation of lipid content in both HDL and LDL particles from blood plasma samples of humans with coronary artery disease. By monitoring the characteristic SRM quantifier ion of each PL category and by adding carbonic anhydrase to plasma samples as an internal standard, quantitation of individual PL levels in both HDL and LDL can be performed separately. Since ionization efficiency of PLs depends on the acyl chain length and the degree of unsaturation, it was difficult to achieve absolute quantitation of PLs using calibration with a few PL standards for the different head groups. However, the addition of a protein standard to the plasma sample is a good alternative for relative quantitation of lipids in lipoproteins. In addition, the current study has the great merit of direct analysis of lipids from human blood samples in aqueous solution without the need for organic solvent extraction of lipids prior to LC-MS/MS analysis, which reduces possible sample loss during sample preparation. There is a possibility of ionization suppression from highly abundant lipid species during the analysis of lipoprotein particles such that it may not be effective to thoroughly screen and quantify low abundant PL species compared to high-resolution separation using nLC-ESI-MS/MS. However, the current method can be utilized to screen abundant lipid species for therapeutic intervention studies of cardiovascular diseases involving HDL/LDL.

Acknowledgements

This study was supported by a grant (No. 2013-035081) from the National Research Foundation (NRF) of Korea funded by the Korean government (MEST).

Appendix A. Supplementary data

Supplementary data associated with this article can be found, in the online version, at <http://dx.doi.org/10.1016/j.chroma.2013.11.035>.

References

- [1] J.C. Giddings, *Science* 260 (1993) 1456.
- [2] K.G. Wahlund, J.C. Giddings, *Anal. Chem.* 59 (1987) 1332.
- [3] S.K. Ratanathanawongs-Williams, in: M.E. Schimpf, K.D. Caldwell, J.C. Giddings (Eds.), *Field-Flow Fractionation Handbook*, Wiley-Interscience, New York, 2000, p. 257.
- [4] P. Reschiglian, M.H.J. Moon, *Proteomics* 71 (2008) 265.
- [5] J.C. Giddings, F.J.F. Yang, M.N. Myers, *Anal. Chem.* 48 (1976) 1126.
- [6] C.A. Converse, E.R. Skinner (Eds.), *Lipoprotein Analysis: A Practical Approach*, Oxford University Press, New York, 1992.
- [7] P.W.F. Wilson, R.B. D'Agostino, D. Levy, A.M. Belanger, H. Silbershatz, W.B. Kannel, *Circulation* 97 (1998) 1837.
- [8] W.E. Boden, *Am. J. Cardiol.* 86 (2000) 19L.
- [9] M.A. Austin, B.L. Rodriguez, B. McKnight, M.J. McNeely, K.L. Edwards, J.D. Curb, D.S. Sharp, *Am. J. Cardiol.* 86 (2000) 412.
- [10] B.A. Griffin, M.J. Caslake, B. Yip, G.W. Tait, C.J. Packard, J. Shepherd, *Atherosclerosis* 83 (1990) 59.
- [11] J. Schiller, O. Zschörnig, M. Petković, M. Müller, J. Arnhold, K. Arnold, *J. Lipid Res.* 42 (2001) 1501.
- [12] S.B. Alabakovska, B.B. Todorova, D.D. Labudovic, K.N. Tosheska, *Clin. Chim. Acta* 317 (2002) 119.
- [13] J. Folch, M. Lees, G.H. Sloane Stanley, *J. Biol. Chem.* 226 (1957) 497.
- [14] E.G. Bligh, W.J. Dyer, *Can. J. Biochem. Physiol.* 37 (1959) 911.
- [15] B. Fuchs, J. Schiller, R. Süß, M. Schürenburg, D. Suckau, *Anal. Bioanal. Chem.* 389 (2007) 827.
- [16] R. Taguchi, J. Hayakawa, Y. Takeuchi, M. Ishida, *J. Mass Spectrom.* 35 (2000) 953.
- [17] G. Isaac, D. Bylund, J.-E. Mansson, K.E. Markides, J. Borgquist, *J. Neurosci. Methods* 128 (2003) 111.
- [18] D.Y. Bang, D. Kang, M.H. Moon, *J. Chromatogr. A* 1104 (2006) 222.
- [19] I. Park, K.J. Paeng, Y. Yoon, J.H. Song, M.H. Moon, *J. Chromatogr. B: Biomed. Sci. Appl.* 780 (2002) 415.
- [20] J.Y. Lee, D. Choi, C. Johan, M.H. Moon, *J. Chromatogr. A* 1218 (2011) 4144.
- [21] D.C. Rambaldi, P. Reschiglian, A. Zattoni, C. Johann, *Anal. Chim. Acta* 654 (2009) 64.
- [22] G. Yohannes, M. Sneek, S.J.O. Varjo, M. Jussila, S.K. Wiedmer, P.T. Kovanen, K. Öörni, M.-L. Riekkola, *Anal. Biochem.* 354 (2006) 255.
- [23] J.Y. Lee, H.K. Min, D.H. Choi, M.H. Moon, *J. Chromatogr. A* 1217 (2010) 1660.
- [24] S.K. Byeon, J.Y. Lee, S. Lim, D. Choi, M.H. Moon, *J. Chromatogr. A* 1270 (2012) 246.
- [25] K.H. Kim, J.Y. Lee, S. Lim, M.H. Moon, *J. Chromatogr. A* 1280 (2013) 92.
- [26] F.-F. Hsu, J. Turk, *J. Am. Soc. Mass Spectrom.* 14 (2003) 352.
- [27] X.C. Jiang, F. Paultre, T.A. Pearson, R.G. Reed, C.K. Francis, M. Lin, L. Berglund, A.R. Tall, *Arterioscler. Thromb. Vasc. Biol.* 20 (2000) 2614.